


Research Article

Substrate Dielectric Constant Effects on the Performances of a Metasurface-Based Circularly Polarized Microstrip Patch Antenna

Kam Eucharist Kedze,¹ Heesu Wang,¹ Yong Bae Park,^{1,2} and Ikmo Park¹ 

¹Department of Electrical and Computer Engineering, Ajou University, Suwon 16499, Republic of Korea

²Department of AI Convergence Network, Ajou University, Suwon 16499, Republic of Korea

Correspondence should be addressed to Ikmo Park; ipark@ajou.ac.kr

Received 4 May 2022; Revised 30 August 2022; Accepted 15 September 2022; Published 30 September 2022

Academic Editor: Lorenzo Crocco

Copyright © 2022 Kam Eucharist Kedze et al. This is an open access article distributed under the Creative Commons Attribution License, which permits unrestricted use, distribution, and reproduction in any medium, provided the original work is properly cited.

This paper presents the effects of substrate dielectric constants on the performance characteristics of a circularly polarized (CP) metasurface-based patch antenna. The antenna structure is a modified patch with a step-like truncation sandwiched between a metasurface composed of a 4×4 lattices of periodic metallic patches and a ground plane. The effects on the performance variations are evaluated for two principal cases that include a uniform dielectric constant and a nonuniform dielectric constant for the upper and lower substrates of the antenna. Through careful computational analysis, the effects of the substrate dielectric constant on the antenna performance in terms of bandwidth and gain were investigated, and the results demonstrate that the antenna performance improves with a decrease in the substrate dielectric constant. For a uniform substrate material with dielectric constants of $\epsilon_{r1} = \epsilon_{r2} = 2.2$, the fabricated antenna with an overall size of $54 \text{ mm} \times 54 \text{ mm} \times 3.0 \text{ mm}$ ($0.76\lambda_0 \times 0.76\lambda_0 \times 0.042\lambda_0$ at 4.24 GHz) demonstrates the following measured performance characteristics: a -10 dB impedance bandwidth of $3.75\text{--}5.24 \text{ GHz}$ (33.14%), a 3 dB axial ratio (AR) bandwidth of $3.85\text{--}4.64 \text{ GHz}$ (18.61%), a radiation efficiency $>93\%$, and a peak gain of 8.96 dBic within the AR bandwidth.

1. Introduction

Nowadays, microstrip patch antennas are commonly used in many wireless communication applications owing to the advantages of being low-profile, lightweight, and low-cost while boasting easy fabrication and ease of integration [1–5]. A conventional microstrip patch antenna generally consists of a printed metallic patch on one side of a dielectric substrate and a ground plane on the other side [6]. The resonance frequency of such antennas is a function of the dimension of the patch and the permittivity and thickness of the substrate. Nonetheless, the principal demerit of microstrip patch antennas is their low performance in terms of narrow bandwidth, which acts as a limitation for many applications [7–12].

The substrate permittivity (ϵ_r) combined with the thickness (h) of a microstrip patch antenna affects the antenna performance characteristics such as resonance

frequency, gain, impedance, and axial ratio (AR) bandwidths [13], and polarization. The substrate, in addition to providing mechanical strength to the overall antenna design, also allows surface waves to propagate through it. High-permittivity substrates reduce the antenna size at the cost of the gain, bandwidth, and cost-effectiveness of the antenna. Accordingly, choosing the most appropriate substrate material with a suitable permittivity is a prime necessity in microstrip antenna design. Because the drawbacks of a microstrip antenna, such as low gain and restricted bandwidth, can be mitigated by selecting suitable substrate materials, the dielectric constant of a substrate is a significant variable in enhancing the gain and bandwidth of a microstrip patch antenna [14, 15].

A metasurface, a two-dimensional counterpart of a metamaterial, is a surface distribution of specially formed subwavelength scattering elements that can shape and control electromagnetic waves [16–20]. The performance of

the metasurfaces is governed by the specific geometrical shape of the scattering elements distributed on the dielectric substrate. These metasurfaces can provide the unique characteristics of an ultra-low profile and enhanced performance in the bandwidth, gain, radiation pattern, and polarization state of the antenna [21–23]. In this paper, we present the effects of the substrate dielectric constant on antenna performance, particularly the bandwidth and radiation gain of a single-feed step-like truncated patch antenna loaded with a metasurface sandwiched between two dielectric substrates. The effects on the antenna performance are evaluated in two categories of dielectric substrates that include uniform and nonuniform dielectric constants. The results demonstrate that the antenna performance increases with decreasing permittivity. The antenna designed with the same dielectric material ($\epsilon_{r1} = \epsilon_{r2} = 2.2$) for both the lower and upper substrates are fabricated and measured, and attained the following performance: An impedance bandwidth for $|S_{11}| \leq -10$ dB of 3.75–5.24 GHz (33.14%), a 3 dB AR bandwidth of 3.85–4.64 GHz (18.61%), a radiation efficiency $>93\%$, and a peak gain of 8.96 dBic within the AR bandwidth at an antenna size of $54 \text{ mm} \times 54 \text{ mm} \times 3.0 \text{ mm}$ ($0.76\lambda_0 \times 0.76\lambda_0 \times 0.042\lambda_0$ at 4.24 GHz).

2. Antenna Geometry

The geometry of the proposed antenna is shown in Figure 1. The antenna consists of a driven patch, metasurface, ground plane, 50Ω SMA connector, and two dielectric substrates with the same thickness of h_1 and h_2 and dielectric constants of ϵ_{r1} and ϵ_{r2} , respectively. The metasurface is a 4×4 lattices of square patches printed on the top surface of the upper substrate with periodicity $P = 13 \text{ mm}$ and a gap between the patches $g = 0.2 \text{ mm}$.

The size of the metasurface unit cell and the number of unit cells constituting the metasurface determine the surface wave resonant frequency of the metasurface [25, 26]. The surface wave resonant frequency of the metasurface according to the size and number of metasurface unit cells can be obtained using a dispersion diagram. Figure 2 is a dispersion diagram according to the design parameter P of a unit cell with $g = 0.2 \text{ mm}$ with $\epsilon_{r1} = \epsilon_{r2} = 2.20$ and $h_1 = h_2 = 1.575 \text{ mm}$ substrate. Figure 2(a) is the 1st mode and 2(b) is the 2nd mode. It can be seen that the 3×3 metasurfaces with $P = 15 \text{ mm}$, the 4×4 metasurface with $P = 13 \text{ mm}$, and the 5×5 metasurfaces with $P = 11 \text{ mm}$ have almost the same surface wave resonant frequency. Figure 3 shows the gain and axis ratio of 3×3 , 4×4 , and 5×5 metasurfaces antennas designed to have the same surface wave resonant frequency. The 3×3 metasurfaces antenna with $P = 15 \text{ mm}$ has a low bandgap frequency, which results in a low antenna gain at the center frequency and poor AR characteristics. On the other hand, the 5×5 metasurfaces antenna with $P = 11 \text{ mm}$ has a high antenna gain at the center frequency, but the 3 dB AR band is shifted to a higher frequency, owing to the small size of the unit cell. In this paper, considering fabrication, a 4×4 metasurfaces using

unit cells with $P = 13 \text{ mm}$ and $g = 0.2 \text{ mm}$, which has the best performance at the center frequency when applied to a substrate with $\epsilon_{r1} = \epsilon_{r2} = 2.20$, was selected. The details of the metasurface design and mechanism are presented [24–27]. The radiating element is a square patch with a step-like truncation printed on the top surface of the lower substrate and sandwiched between the metasurface and the ground plane. The outer conductor of the coaxial line is connected to the ground plane, and the inner conductor of the coaxial line extends through the lower substrate to connect to the extended strip of the radiating patch [28]. The extended strip is a stub attached to the driven patch to improve the impedance matching [29]. For different values of ϵ_{r1} and ϵ_{r2} , each antenna was optimized with ANSYS high-frequency simulation software to show the effects of the substrate dielectric constant on the antenna gain, impedance bandwidth, and AR bandwidth.

3. Antenna Performance

To simplify, the effects of the substrate dielectric constant on the antenna performance are summarized into two categories, those of a uniform dielectric constant and those of a nonuniform dielectric constant.

3.1. Uniform Dielectric Constant ($\epsilon_{r1} = \epsilon_{r2}$). In the case of a uniform dielectric constant material, the same dielectric constant is utilized for both the upper and lower substrates. Table 1 shows a summary of the performance variations of the antenna as a function of the antenna's dielectric constant. An observation of the table provides a good understanding of the effects of different dielectric constant substrates on the antenna performance in terms of impedance bandwidth, AR bandwidth, and gain. In the context of impedance bandwidth, it can be seen from the table that the proposed antenna operates with a wide impedance bandwidth when the dielectric constant is 1.06 for both the lower and upper substrates. At this value, the impedance bandwidth generated is 47.55%, as shown in Figure 4. The figure also confirms that when the dielectric constant is changed to a value of 2.2 for both substrates, the dielectric effect is noticeable with a shift in the entire reflection coefficient curve to low frequencies. This shift is also accompanied by a nearly 15% reduction in the impedance bandwidth. Similarly, at a dielectric constant of 3.38, the $|S_{11}|$ curve shifts more toward lower frequencies compared with the aforementioned case and demonstrates an increased reduction in the impedance bandwidth of approximately 18%.

In the context of the AR bandwidth, the proposed antenna with a dielectric constant of 1.06 for both substrates generates a broad AR bandwidth of 21.5% with two AR minimum points. The first minimum point is generated by the patch whereas the second minimum point is generated from the metasurface [26]. In all three cases, exactly the same number of AR minimum points is generated, as shown in Figure 5. Nevertheless, different AR bandwidths are produced, as seen in Table 1. When the dielectric constant is

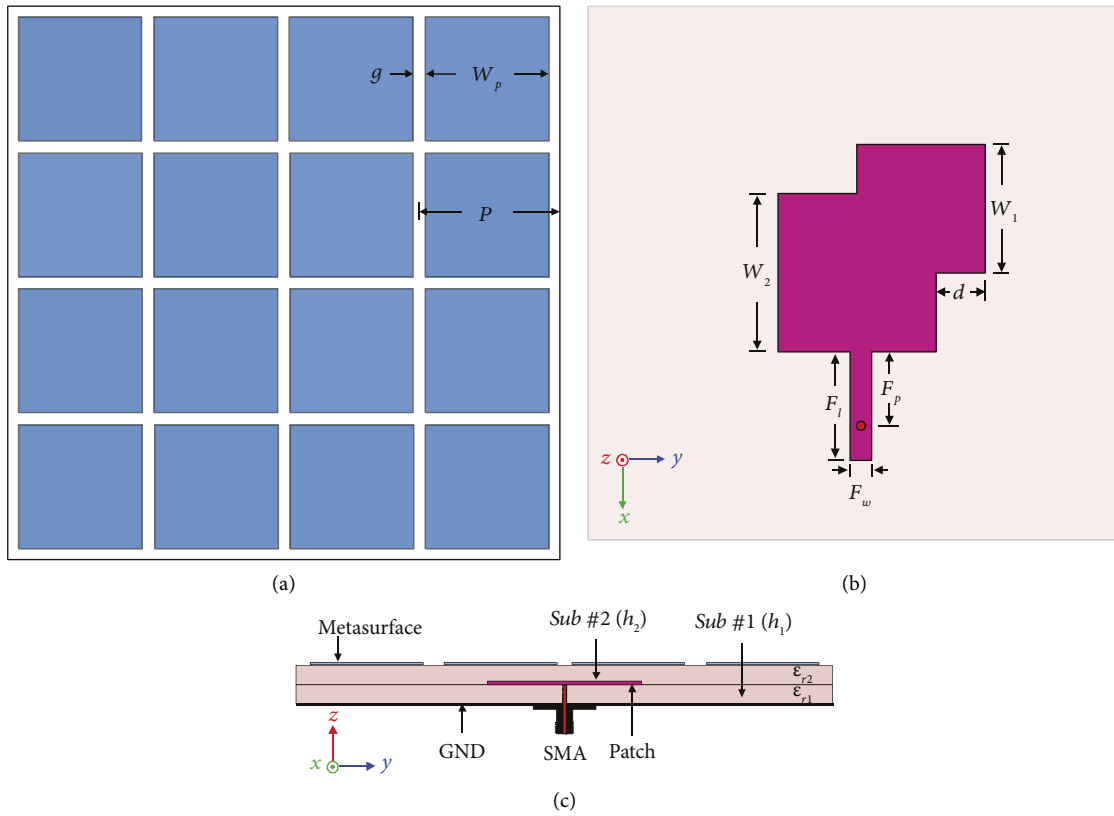


FIGURE 1: Geometry of the proposed antenna: (a) top view, (b) top view of driven patch, and (c) side view.

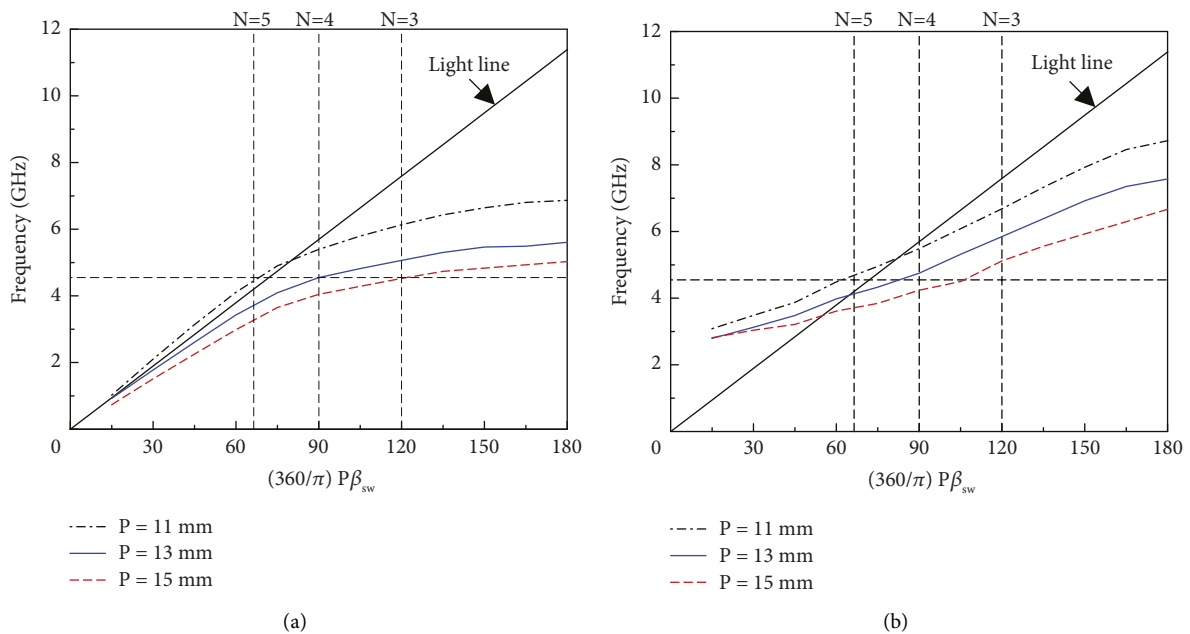


FIGURE 2: Dispersion diagram of a unit cell with $g=0.2$ mm: (a) 1st mode and (b) 2nd mode.

changed from a low value of 1.06 to a high value of 2.2 for all substrates, a shift towards low frequencies is observed with a slight reduction in the AR bandwidth. When the dielectric constant is 3.38, more shifts are achieved, but the reduction in AR bandwidth almost remains the same.

The aforementioned results of the reflection coefficient and AR show the same trend with changes in the dielectric constant for both substrates. The first significant trend is the shift of the $|S_{11}|$ and AR curves to low frequencies with increasing dielectric constant. An increase in the dielectric

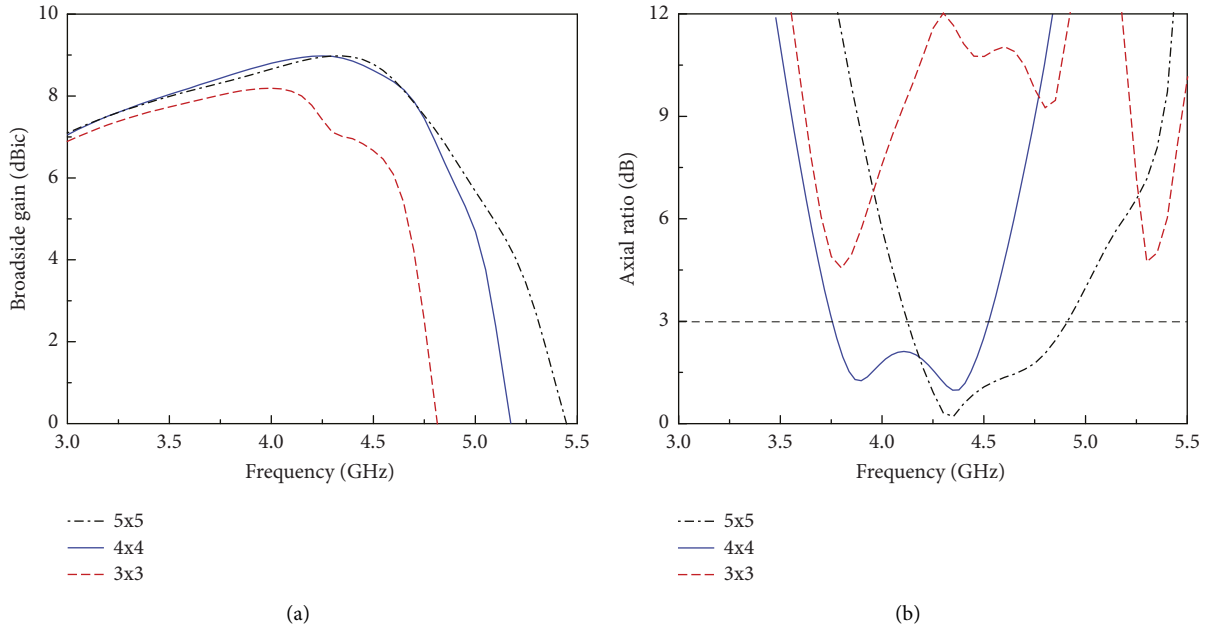


FIGURE 3: Characteristics of 3×3 , 4×4 , and 5×5 metasurfaces antennas: (a) gain and (b) AR.

TABLE 1: Performance summary of the antenna with the same dielectric constants for both the lower and upper substrates.

Lower substrate dielectric constant, ϵ_{r1}	Upper substrate dielectric constant, ϵ_{r2}	Antenna size (λ_0^3)	$ S_{11} \leq -10$ BW (%)	AR BW (%)	Peak gain (dBic)
1.06	1.06	$0.98 \times 0.98 \times 0.054$	47.55 (4.68–7.6 GHz)	21.5 (4.9–6.08 GHz)	10.5
2.2	2.2	$0.76 \times 0.76 \times 0.042$	33.14 (3.75–5.24 GHz)	18.61 (3.85–4.64 GHz)	8.96
3.38	3.38	$0.69 \times 0.69 \times 0.038$	30.4 (3.48–4.73 GHz)	17.89 (3.51–4.2 GHz)	7.88

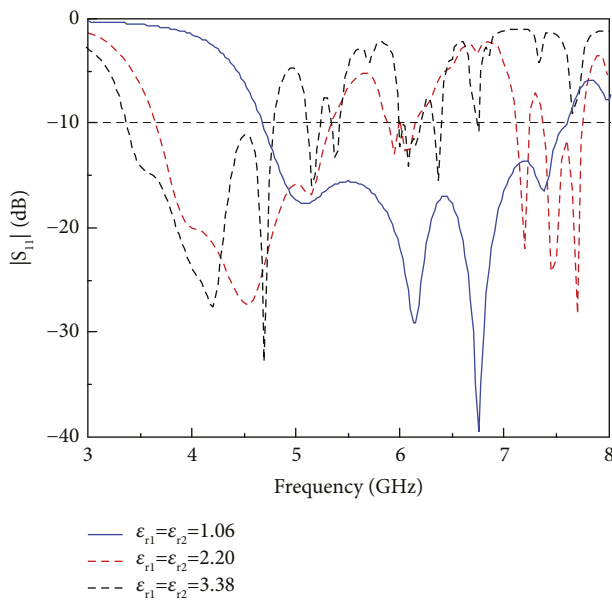


FIGURE 4: Effects of the substrate dielectric constant on the reflection coefficient of the antenna.

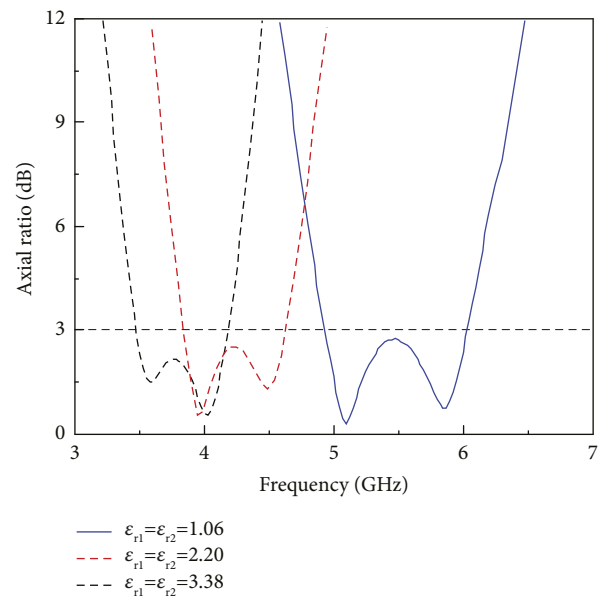


FIGURE 5: Effects of the substrate dielectric constant on the AR of the antenna.

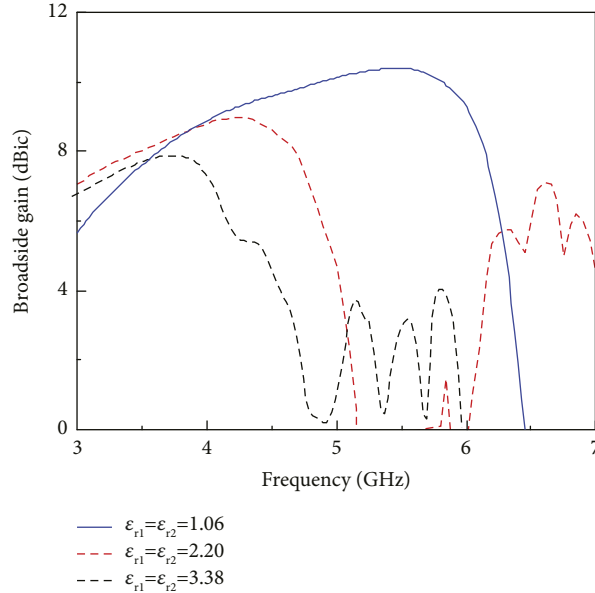


FIGURE 6: Effects of the substrate dielectric constant on the broadside gain of the antenna.

TABLE 2: Performance summary of the antenna with different dielectric constants for both the lower and upper substrates.

Lower substrate dielectric constant, ϵ_{r1}	Upper substrate dielectric constant, ϵ_{r2}	Antenna size (λ_0^3)	$ S_{11} \leq -10$ BW (%)	AR BW (%)	Peak gain (dBic)
1.06	2.2	$0.82 \times 0.82 \times 0.046$	44.54 (4.1–6.45)	17.39 (4.2–5.0)	9.31
2.2	1.06	$0.91 \times 0.91 \times 0.051$	36.6 (4.52–6.55)	19.55 (4.66–5.67)	10.16
1.06	3.38	$0.73 \times 0.73 \times 0.040$	25.9 (3.73–4.84)	14.47 (3.78–4.37)	8.46
3.38	1.06	$0.82 \times 0.82 \times 0.046$	17.39 (4.2–5.0)	17.39 (4.2–5.0)	9.69

constant produces an increase in the effective patch size or radius that results in a corresponding shift to low frequencies. Another notable trend is the reduction of bandwidth with an increasing dielectric constant. The deterioration in bandwidth can be attributed to the increased total quality factor and a decrease in the fringing fields as the dielectric constant increases.

The predominant effect of the dielectric constant on the antenna performance is shown in Figure 6, which shows the gain of the antenna as a function of frequency for different dielectric constants. It is evident from both Figure 6 and Table 1 that with low dielectric constant values such as 1.06 for the lower and upper substrates, high gain values above 10.0 dBic are achievable. When the dielectric constant value increases, the expected shift to low frequencies is exhibited; however, the radiation gain deteriorates accordingly. For instance, when the dielectric constant is changed from 1.06 to 2.2, the gain drops from 10.5 dBic to 8.96 dBic, which is equivalent to a decrease of approximately 1.5 dBic. Therefore, decreasing the dielectric constants for both substrates generate increasing gain and vice versa. The rise in gain at a low dielectric constant is because the patch size at resonance increases electrically, and consequently, the radiating area eventually enhances the antenna gain. Furthermore, the dielectric substrate provides a medium for the propagation of surface waves that deplete some of the power available for

radiation, reducing the radiation gain. With high dielectric constant materials, there are increased dielectric losses and reduced gain values.

3.2. Nonuniform Dielectric Constant ($\epsilon_{r1} \neq \epsilon_{r2}$). A combination of substrates with different permittivities for the lower and upper substrates is employed in the antenna with nonuniform dielectric constants. The performance of the antenna is evaluated with the lower and upper substrates having different dielectric constants in one case, and then, swapping the dielectric constants of the lower and upper substrates in the other case. Therefore, two pairs of dielectric constants are considered. The first pair consists of dielectric constant values of 1.06 and 2.20. In Table 2, the first row assigns $\epsilon_{r1} = 1.06$ for the lower substrate and $\epsilon_{r2} = 2.20$ for the upper substrate. This particular case generates a wide impedance bandwidth of 44.54% and an appreciable AR bandwidth of 17.39% with a moderate electrical size of the antenna. The generated gain values are also high with a peak value of 9.31 dBic. In row 2 of Table 2, the dielectric constants of row 1 are swapped, and the lower substrate has a dielectric constant of $\epsilon_{r1} = 2.20$, whereas the upper substrate has a dielectric constant of $\epsilon_{r2} = 1.06$. Compared with the preceding case, the antenna shows a reduction in the impedance bandwidth with other improvements demonstrated

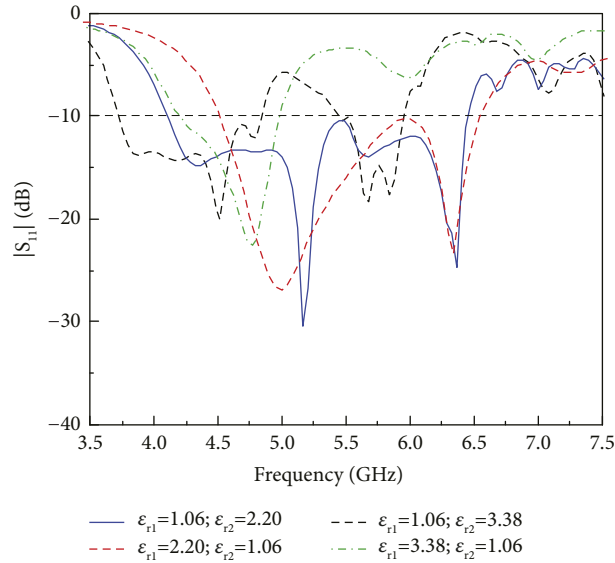


FIGURE 7: Effects of different dielectric constants for the lower and upper substrates on the reflection coefficient of the antenna.

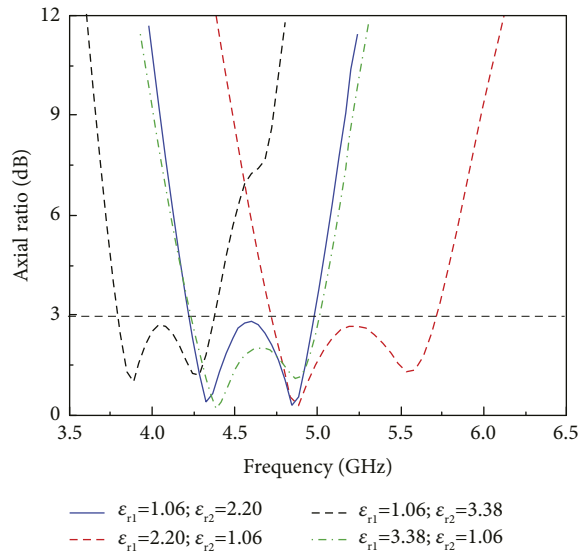


FIGURE 8: Effects of different dielectric constants for the lower and upper substrates on the axial ratio of the antenna.

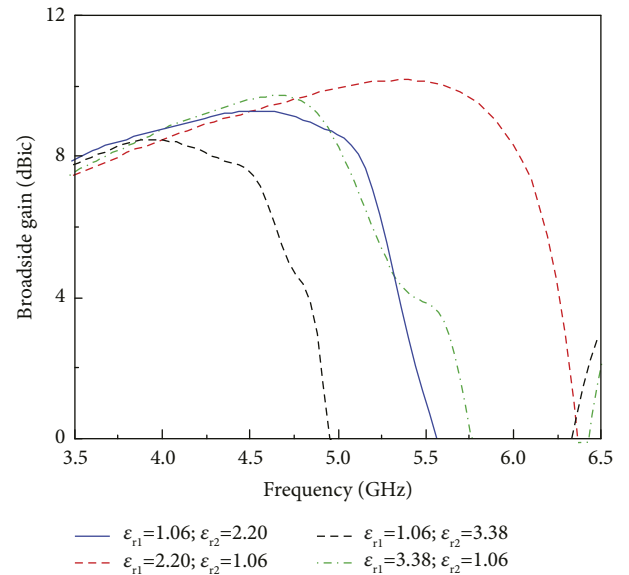


FIGURE 9: Effects of different dielectric constants for the lower and upper substrates on the broadside gain of the antenna.

by a slight increment in the AR bandwidth and broadside gain. Therefore, with $\epsilon_{r1}=2.20$ and $\epsilon_{r2}=1.06$, the antenna shows a better useable CP bandwidth and gain values above 10.0 dBic. From Figure 7, which shows the reflection coefficient profile of the different dielectric constant combinations, the $|S_{11}|$ with $\epsilon_{r1}=1.06$ and $\epsilon_{r2}=2.2$ demonstrates multiple resonances within its profile that produce a wider bandwidth compared with the $|S_{11}|$ with $\epsilon_{r1}=2.20$ and $\epsilon_{r2}=1.06$ that shows just two resonances. This is because surface waves are strongly excited within the metasurface and produce better impedance bandwidth when the upper substrate has a dielectric constant of $\epsilon_{r2}=2.2$. Figure 8 shows the AR of the antenna with various dielectric constant combinations. The figure visibly compares the AR profiles and shows two AR minimum points and a shift of

approximately 0.6 GHz between the AR curves for $\epsilon_{r1}=2.20$ and $\epsilon_{r2}=1.06$, and $\epsilon_{r1}=2.20$ and $\epsilon_{r2}=1.06$. The shifting or movement along the frequency scale in the figure is because both the aforementioned cases have the same physical patch size but different electrical and effective sizes. The gain curves of the different dielectric constant combinations are represented in Figure 9. It can be observed that the case with $\epsilon_{r1}=2.20$ and $\epsilon_{r2}=1.06$ produces higher gain values than the case with these dielectric constants interchanged. When the upper substrate with the printed metasurface has the lower dielectric constant of 1.06, the effective size of the metasurface is increased, giving rise to a larger effective aperture area that improves the antenna gain. In contrast, when the upper substrate has a higher dielectric constant of 2.2, there

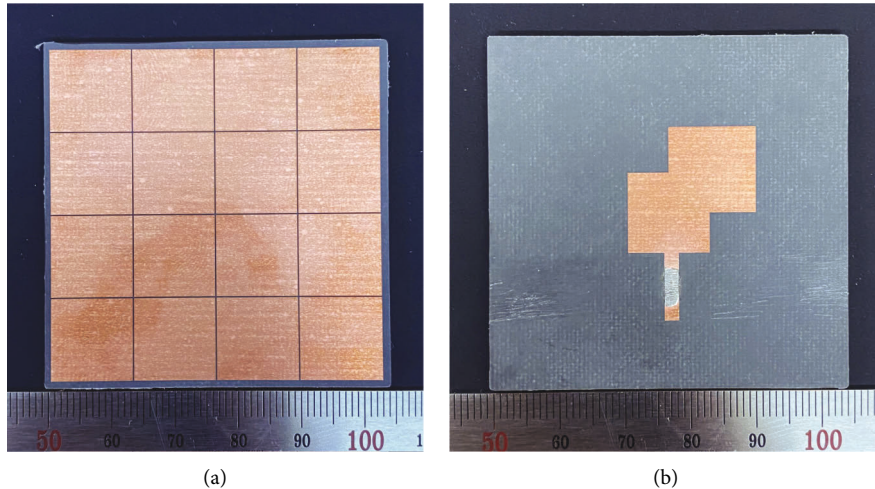


FIGURE 10: Fabricated sample of the antenna with $\epsilon_{r1} = \epsilon_{r2} = 2.20$: (a) top view of metasurface and (b) top view of the driven patch.

is an increase in the dielectric losses and a high propagation loss of the surface waves within the dielectric medium that reduces the radiation gain.

In Table 2, the second pair of dielectric constant values are 1.06 and 3.38. The main advantage obtained by employing $\epsilon_{r1} = 1.06$ and $\epsilon_{r2} = 3.38$ is the reduction in the electrical size of the antenna, which is accompanied by a reduction in the useable CP bandwidth of the antenna. Nonetheless, in the inverse situation with $\epsilon_{r1} = 3.38$ and $\epsilon_{r2} = 1.06$, the antenna size is reduced without significantly losing the useable CP bandwidth and high gain values are produced by the antenna. By using combinations of dielectric constant values and interchanging their positions, the antenna size is reduced without considerable loss in performance. For example, in the case with $\epsilon_{r1} = 2.20$ and $\epsilon_{r2} = 1.06$, the electrical size is reduced while the bandwidth is nearly maintained at the optimum level and the gain values are above 10.0 dBic.

4. Experimental Setup

Figure 10 shows a prototype that was fabricated and measured with a dielectric constant of 2.2 for both the top and bottom substrates. The antenna was etched on a Roger 5880 substrate with a height $h_1 = h_2 = 1.5748$ mm and with the following design parameters: $g = 0.2$ mm, $P = 13$ mm, $W_p = 12.8$ mm, $W_1 = 14$ mm, $W_2 = 12.5$ mm, $d = 7.8$ mm, $F_p = 4.6$ mm, $F_1 = 10.5$ mm, and $F_w = 2.2$ mm. To measure the reflection coefficient of the antenna, an Agilent E8362B Network Analyzer and a 3.5 mm Coaxial Calibration Standard (GCS35M) were used. The measured reflection coefficient showed consistency with the simulated results that ranged from 3.66 to 5.23 GHz with an impedance bandwidth of 35.32%. Figure 11 is a graph of the simulated and measured reflection coefficients. For far-field radiation pattern measurements, a full anechoic chamber with dimensions of 5.5 m (W) \times 5.5 m (L) \times 5.0 m (H) at the Electromagnetic Wave Technology Institute (EMTI) Yongsan, Korea was utilized. During the radiation pattern measurement process, a standard wideband horn antenna was used for transmission while the fabricated antennas were used for reception. The

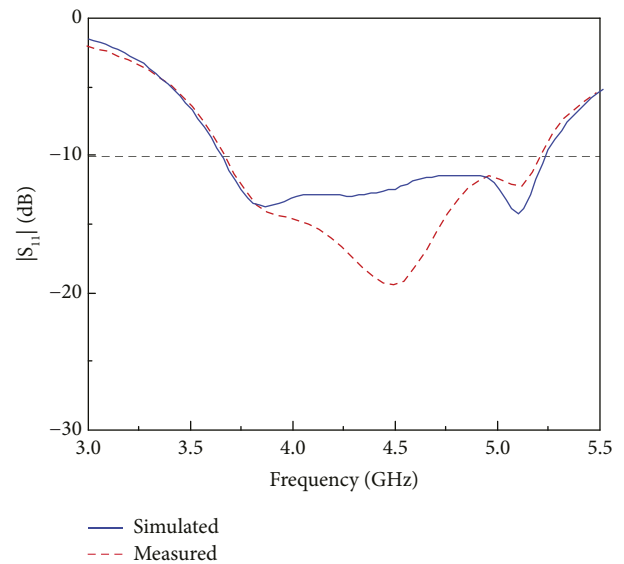


FIGURE 11: Simulated and measured reflection coefficient of the antenna.

transmitter-receiver separation distance was 2.9 m. The horn antenna was fixed while the fabricated antenna was rotated from -180° to 180° at a scan angle of 1° and a speed of 3° s^{-1} . The AR, broadside gain, and radiation patterns were measured and recorded. The measured AR in the broadside direction as shown in Figure 12 ranges from 3.72 to 4.55 GHz and exactly overlaps the simulated AR with an AR bandwidth of 20.07%. The measured broadside gain shows the same profile as the simulated gain. Both the measured gain and simulated gain have a peak gain of 8.89 dBic, as presented in Figure 13. The radiation patterns were measured at two frequency points of 3.9 GHz and 4.35 GHz and plotted in Figure 14. The measurements indicate that the antenna produced good broadside unidirectional left-hand (LH) CP radiation patterns that are identical to their simulated counterparts. The measured patterns showed good symmetry in both the xz - and yz -planes.

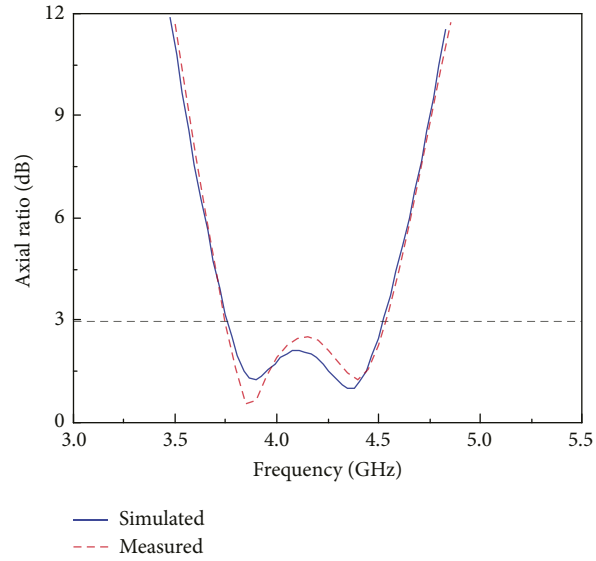


FIGURE 12: Simulated and measured axial ratio of the antenna.

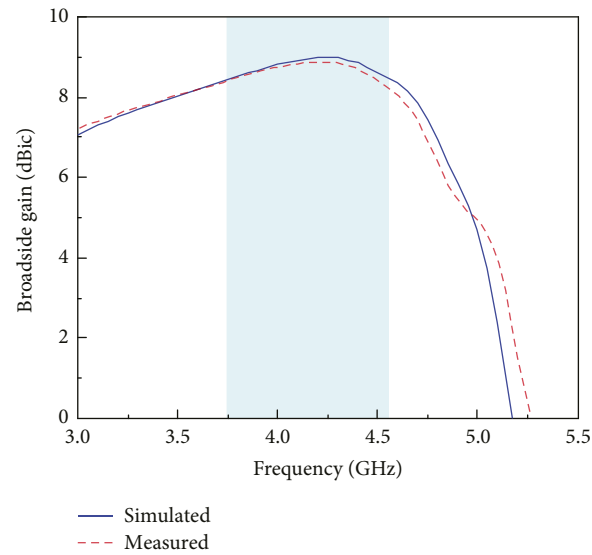
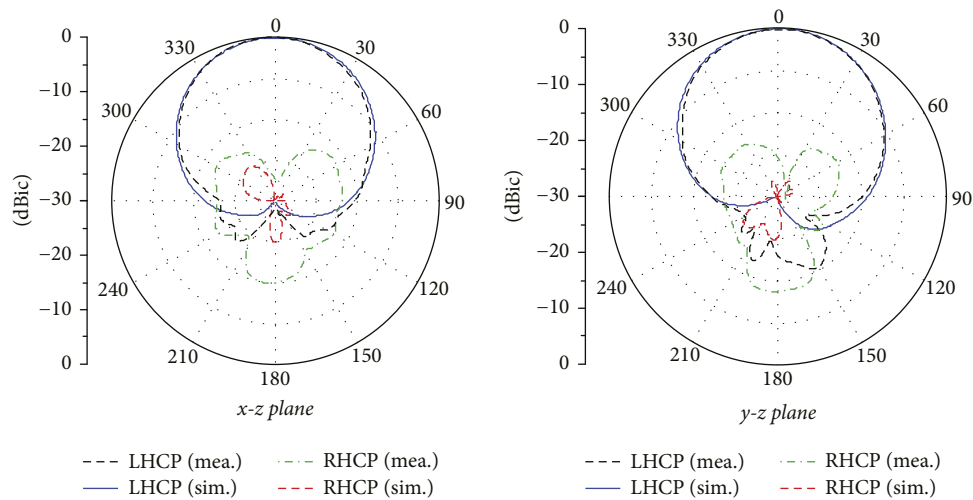


FIGURE 13: Simulated and measured broadside gain of the antenna.



(a)

FIGURE 14: Continued.

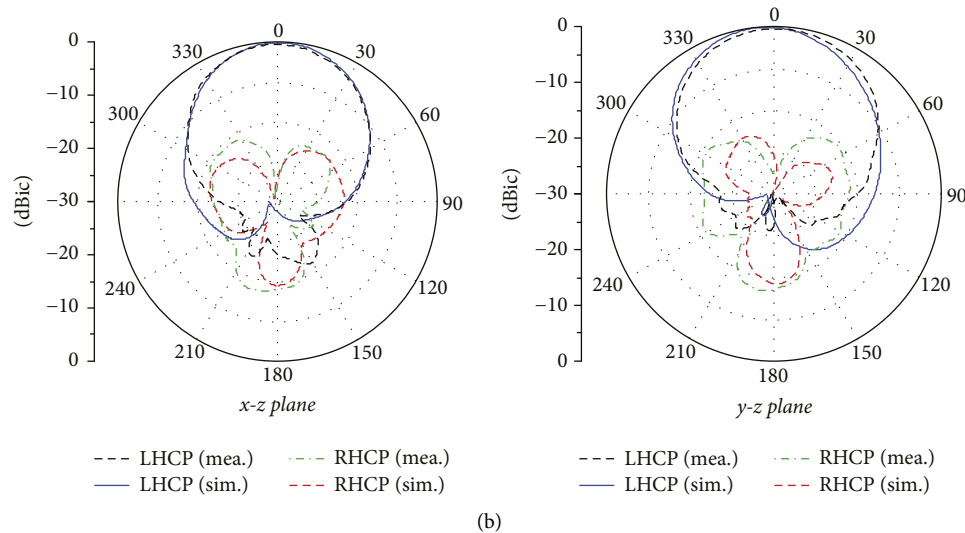


FIGURE 14: Simulated and measured radiation patterns of the antenna: (a) 3.9 GHz and (b) 4.35 GHz.

5. Conclusions

In this paper, the effects of the substrate dielectric constant on the performance of a modified square patch with a step-like truncation incorporated into the metasurface are presented. A concise and comprehensive study on the effects of the substrate dielectric constant on the antenna performance is demonstrated. The analysis establishes that the substrate dielectric constant has a significant effect on the antenna performance. With decreasing dielectric constant, the antenna performance is improved. Furthermore, by using substrates with different combinations of permittivity, the antenna size is reduced without significant degradation in antenna performance. A sample antenna is fabricated and measured with a low dielectric constant of 2.2 for both the top and bottom substrates for verification. The antenna showed a high gain with a peak value of 8.96 dBic and produced symmetrical LHCP unidirectional radiation patterns. The antenna has the merits of a low cross-polarization level, high gain, and wide bandwidth with a low profile.

Data Availability

All the data are included within the manuscript.

Conflicts of Interest

The authors declare that they have no conflicts of interest.

Acknowledgments

This work was supported in part by the Basic Science Research Program through the National Research Foundation of Korea (NRF) funded by the Ministry of Education (NRF-2022R1F1A1065324); in part by the National Research Foundation of Korea (NRF) grant funded by the Korea government (MSIT) (No. 2021R1A4A1030775); and in part by the Institute of Information & communications

Technology Planning & Evaluation (IITP) grant funded by the Korea government (MSIT) (No. 2022-0-00704-001, Development of 3D-NET Core Technology for High-Mobility Vehicular Service).

References

- [1] D. Rano, M. A. Chaudhary, and M. S. Hashmi, "A new model to determine effective permittivity and resonant frequency of patch antenna covered with multiple dielectric layers," *IEEE Access*, vol. 8, pp. 34418–34430, 2020.
- [2] W. Liu, Z. N. Chen, and X. Qing, "Metamaterial-based low-profile broadband aperture-coupled grid-slotted patch antenna," *IEEE Transactions on Antennas and Propagation*, vol. 63, no. 7, pp. 3325–3329, July 2015.
- [3] W. Liu, Z. N. Chen, and X. Qing, "Metamaterial-based low-profile broadband mushroom antenna," *IEEE Transactions on Antennas and Propagation*, vol. 62, no. 3, pp. 1165–1172, 2014.
- [4] Z. Liang, J. Ouyang, and F. Yang, "Low-profile wideband circularly polarised single-layer metasurface antenna," *Electronics Letters*, vol. 54, no. 24, pp. 1362–1364, 2018.
- [5] S. X. Ta and I. Park, "Compact wideband circularly polarized patch antenna array using metasurface," *IEEE Antennas and Wireless Propagation Letters*, vol. 16, pp. 1932–1936, 2017.
- [6] J. W. Salman, M. M. Ameen, and S. O. Hassan, "Effects of the loss tangent, dielectric substrate permittivity and thickness on the performance of circular microstrip antennas," *Journal of Engineering and Development*, vol. 10, no. 1, pp. 1–13, Mar. 2006.
- [7] X. Zhang and L. Zhu, "High-gain circularly polarized microstrip patch antenna with loading of shorting pins," *IEEE Transactions on Antennas and Propagation*, vol. 64, no. 6, pp. 2172–2178, June 2016.
- [8] Z. Wang, J. Liu, and Y. Long, "A simple wide-bandwidth and high-gain microstrip patch antenna with both sides shorted," *IEEE Antennas and Wireless Propagation Letters*, vol. 18, no. 6, pp. 1144–1148, June 2019.
- [9] Y. Cao, Y. Cai, W. Cao et al., "Broadband and high-gain microstrip patch antenna loaded with parasitic mushroom-type structure," *IEEE Antennas and Wireless Propagation Letters*, vol. 18, no. 7, pp. 1405–1409, July 2019.

- [10] X. Zhang and L. Zhu, "Gain-enhanced patch antenna without enlarged size via loading of slot and shorting pins," *IEEE Transactions on Antennas and Propagation*, vol. 65, no. 11, pp. 5702–5709, 2017.
- [11] X. Zhang and L. Zhu, "Gain-enhanced patch antennas with loading of shorting pins," *IEEE Transactions on Antennas and Propagation*, vol. 64, no. 8, pp. 3310–3318, 2016.
- [12] R. Q. Lee and K. F. Lee, "Experimental study of the two-layer electromagnetically coupled rectangular patch antenna," *IEEE Transactions on Antennas and Propagation*, vol. 38, no. 8, pp. 1298–1302, 1990.
- [13] J. H. Kim and B. G. Kim, "Effect of feed substrate thickness on the bandwidth and radiation characteristics of an aperture-coupled microstrip antenna with a high permittivity feed substrate," *Journal of Electromagnetic Engineering and Science*, vol. 18, no. 2, pp. 101–107, Apr. 2018.
- [14] K. P. Kumar, K. S. Rao, V. M. Rao, K. Uma, A. Somasekhar, and C. M. Mohan, "The effect of dielectric permittivity on radiation characteristics of co-axially feed rectangular patch antenna: design & Analysis," *International Journal of Advanced Research in Computer and Communication Engineering*, vol. 2, pp. 1254–1258, 2013.
- [15] A. Thakur, M. Chauhan, and M. Kumar, "Effect of substrate relative dielectric constant on bandwidth characteristics of line feed rectangular patch antenna," *International Journal of Engineering Science Invention Research & Development*, vol. 1, pp. 391–396, Apr. 2015.
- [16] C. L. Holloway, E. F. Kuester, J. A. Gordon, J. O'Hara, J. Booth, and D. R. Smith, "An overview of the theory and applications of metasurfaces: the two-dimensional equivalents of metamaterials," *IEEE Antennas and Propagation Magazine*, vol. 54, no. 2, pp. 10–35, Apr. 2012.
- [17] A. Li, S. Singh, and D. Sievenpiper, "Metasurfaces and their applications," *Nanophotonics*, vol. 7, no. 6, pp. 989–1011, 2018.
- [18] N. Yu, P. Genevet, M. A. Kats et al., "Light propagation with phase discontinuities: generalized laws of reflection and refraction," *Science*, vol. 334, no. 6054, pp. 333–337, 2011.
- [19] H. H. Hsiao, C. H. Chu, and D. P. Tsai, "Fundamentals and applications of metasurfaces," *Small Methods*, pp. 1–20, Article ID 1600064, 2017.
- [20] S. B. Glybovski, S. A. Tretyakov, P. A. Belov, Y. S. Kivshar, and C. R. Simovski, "Metasurfaces: from microwaves to visible," *Physics Reports*, vol. 634, pp. 1–72, 2016.
- [21] I. Park, "Application of metasurfaces in the design of performance-enhanced low-profile antennas," *EPJ Applied Metamaterials*, vol. 5, no. 11, pp. 11–13, 2018.
- [22] Y. Dong and T. Itoh, "Metamaterial-based antennas," *Proceedings of the IEEE*, vol. 100, no. 7, pp. 2271–2285, 2012.
- [23] B. Ratni, E. Bochkova, G. P. Piau, A. de Lustrac, A. Lupu, and S. N. Burokur, "Design and engineering of metasurfaces for high-directivity antenna and sensing applications," *EPJ Applied Metamaterials*, vol. 3, no. 4, pp. 4–10, 2016.
- [24] K. E. Kedze, H. Wang, and I. Park, "A metasurface-based wide-bandwidth and high-gain circularly polarized patch antenna," *IEEE Transactions on Antennas and Propagation*, vol. 70, no. 1, pp. 732–737, Jan. 2022.
- [25] S. X. Ta and I. Park, "Artificial magnetic conductor-based circularly polarized crossed-dipole antennas: 1. AMC structure with grounding pins," *Radio Science*, vol. 52, no. 5, pp. 630–641, May 2017.
- [26] S. X. Ta and I. Park, "Artificial magnetic conductor-based circularly polarized crossed-dipole antennas: 2. AMC structure without grounding pins," *Radio Science*, vol. 52, no. 5, pp. 642–652, May 2017.
- [27] S. Nelaturi and N. V. S. N. Sarma, "A compact microstrip patch antenna based on metamaterials for Wi-Fi and WiMAX applications," *Journal of Electromagnetic Engineering and Science*, vol. 18, no. 3, pp. 182–187, July 2018.
- [28] K. E. Kedze, H. Wang, and I. Park, "Effects of split position on the performance of a compact broadband printed dipole antenna with split-ring resonators," *Journal of Electromagnetic Engineering and Science*, vol. 19, no. 2, pp. 115–121, Apr. 2019.
- [29] S. X. Ta and I. Park, "Low-profile broadband circularly polarized patch antenna using metasurface," *IEEE Transactions on Antennas and Propagation*, vol. 63, no. 12, pp. 5929–5934, 2015.